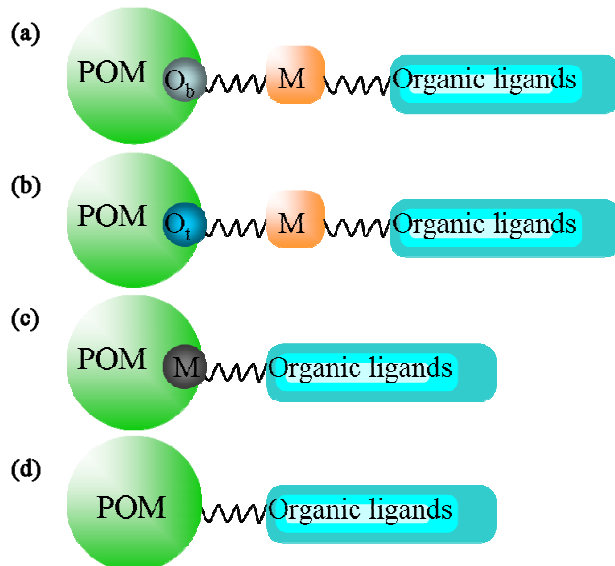


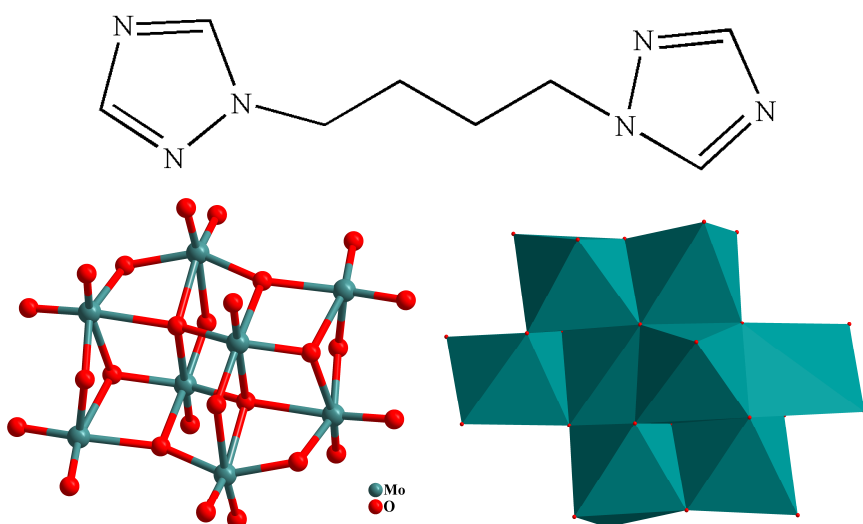
## A 3D organopolymolybdate polymer with unusual topology functionalized by 1,4-bis(1,2,4-triazol-1-yl)butane through Mo-N bond†

Xiuli Wang,\* Jin Li, Aixiang Tian, Guocheng Liu, Qiang Gao, Hongyan Lin and Dan Zhao

Faculty of Chemistry and Chemical Engineering, Bohai University, Jinzhou, 121000, P.R. China..



**Scheme S1.** Schematic representation of the synthesis strategies for POM-based hybrids. M: transition metal ions; O<sub>b</sub>: bridging O atoms; O<sub>t</sub>: terminal O atoms.



**Scheme S2.** Organic ligand (**L**) and  $\gamma\text{-Mo}_8\text{O}_{26}^{4-}$  anion used in this report.

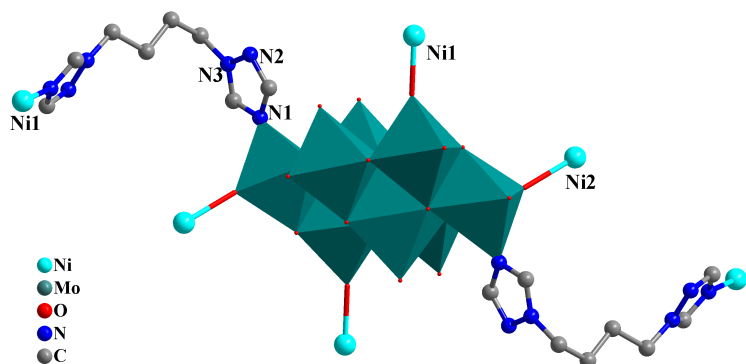


**Fig. S1.** Ball-and-stick and polyhedral representation of  $\gamma$ - $\text{Mo}_8\text{O}_{26}$  anion functionalized by **L** ligand.

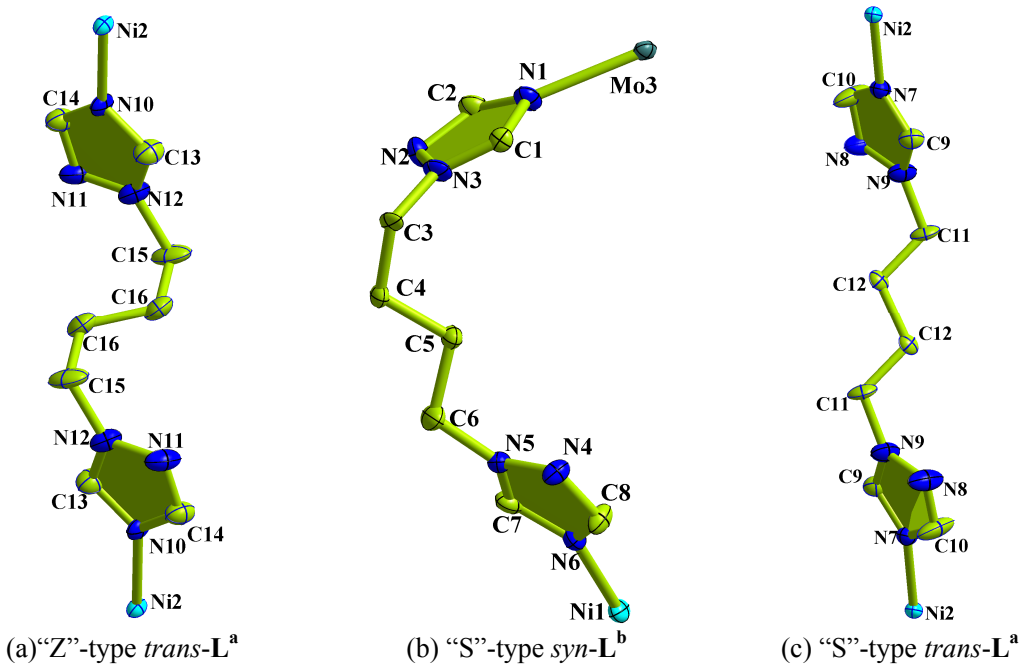


**Fig. S2.** Two types of **L** ligands with different coordination modes (**L**<sup>a</sup> and **L**<sup>b</sup>) exhibiting three conformation in **1**.

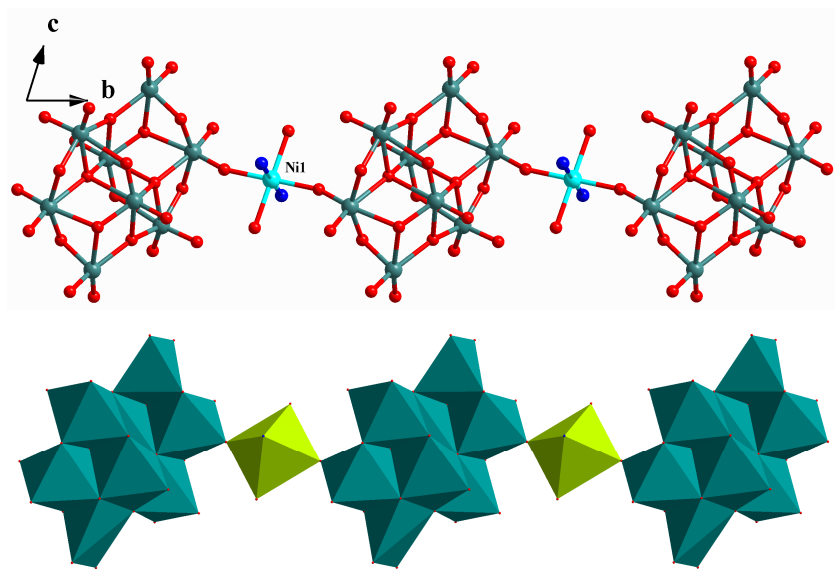


**Fig. S3.** Ball-and-stick (up) and polyhedral (down) representations of the 1D infinite inorganic chain along *b* axis.

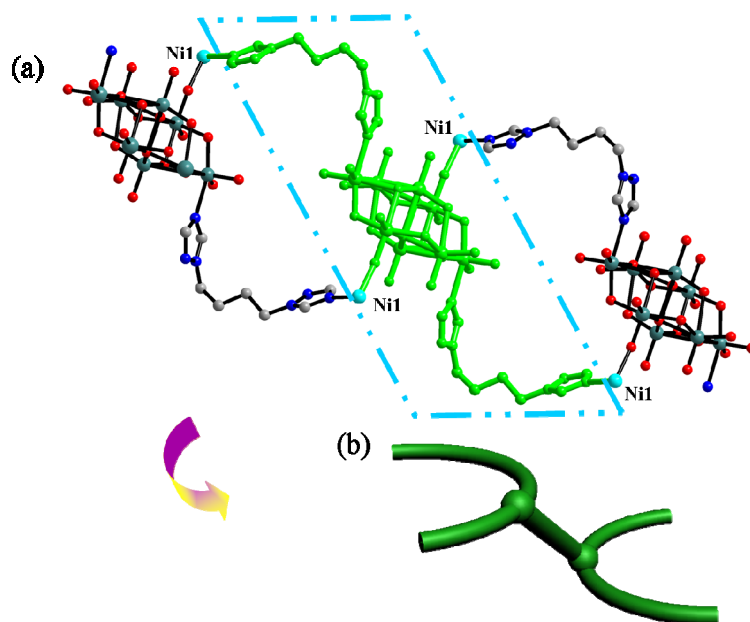


**Fig. S4.** Ball-and-stick representation (a) and schematic view (b) of the bridging double semi-circles motif (A) in **1**.

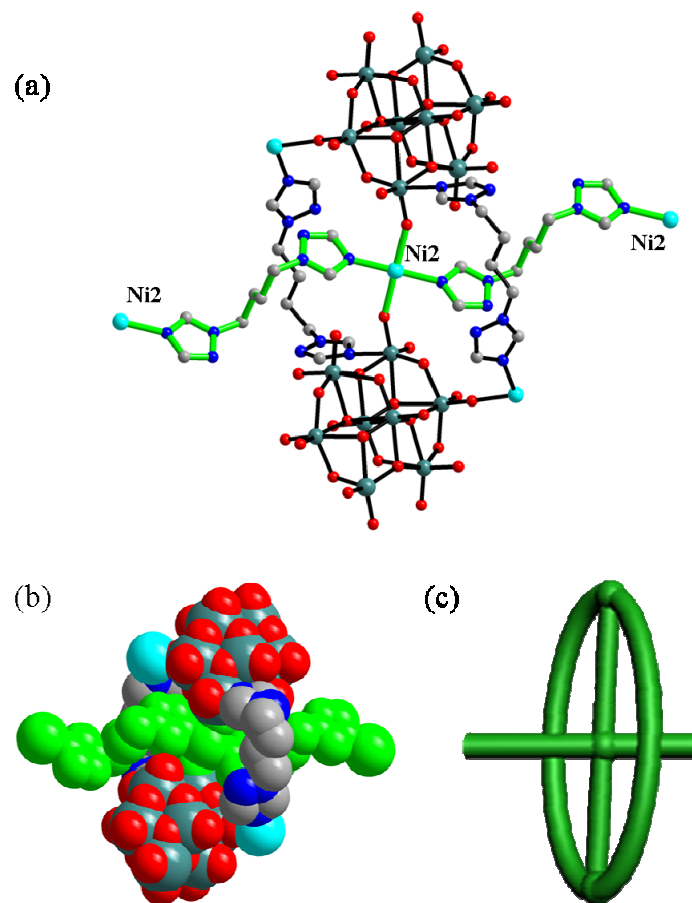


**Fig. S5.** Ball-and-stick representation (a), spacefilling representation (b) and schematic view (c) of the self-threading motif (B) in **1**.

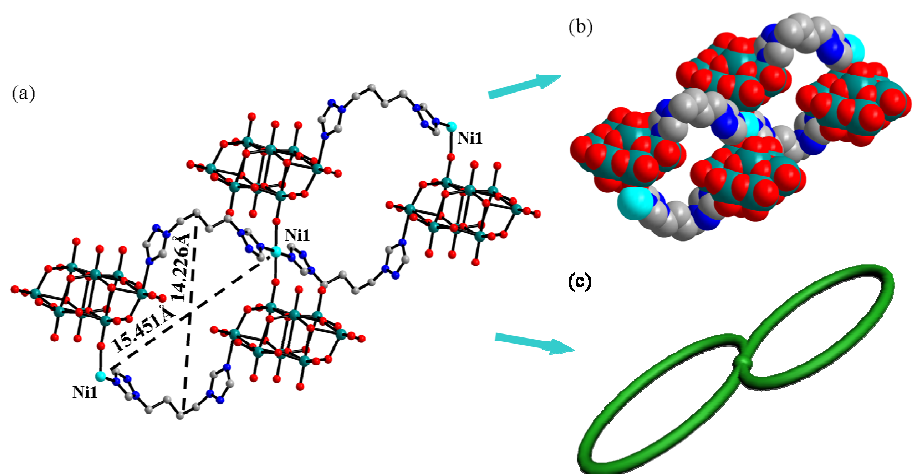


**Fig. S6.** Ball-and-stick representation (a), spacefilling representation (b) and schematic view (c) of the 8-like circle (C) in **1**.

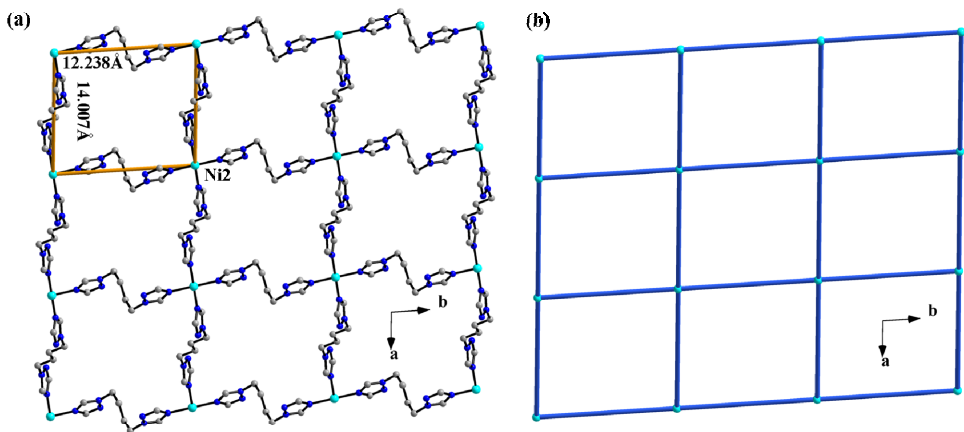


**Fig. S7.** Ball-and-stick representation (a) and schematic view (b) of the 2D sheet-like structure (D) in **1**.

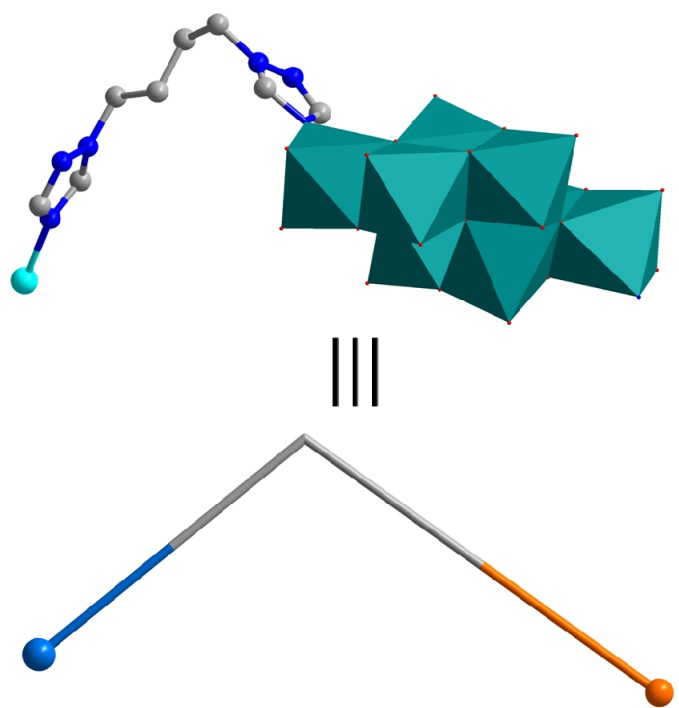


**Fig. S8.** The ligand  $\mathbf{L}^b$  is viewed as spacer in the topology.

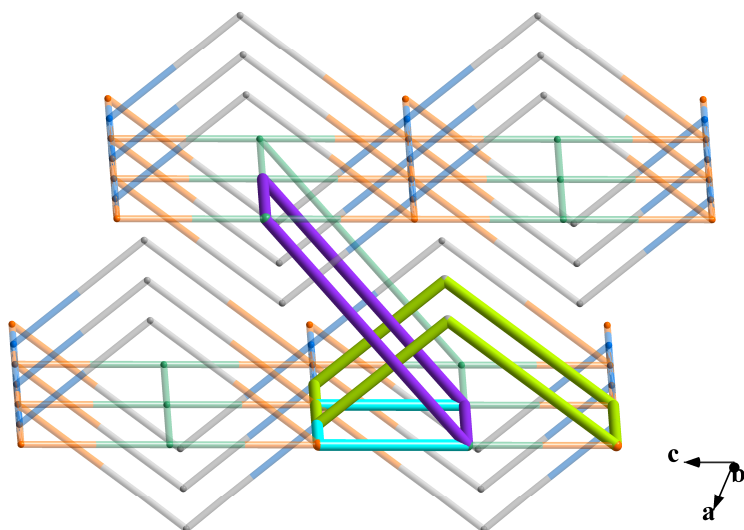


**Fig. S9.** The self-penetrating fragment highlighted by bold lines

The compound **1** bulk-modified carbon paste electrode (**1**-CPE) was fabricated as follows: 0.5 g graphite powder and 0.03 g compound **1** were mixed and ground together by agate mortar and pestle for approximately 30 min to achieve an even, dry mixture; to the mixture 0.15 ml paraffin oil was added and stirred with a glass rod; then the homogenized mixture was used to pack 2 mm inner diameter glass tubes to a length of 0.5 cm. The electrical contact was established with the copper stick, and the surface of the **1**-CPE was wiped with weighing paper. The same procedure was used for preparation of bare CPE without the complex.

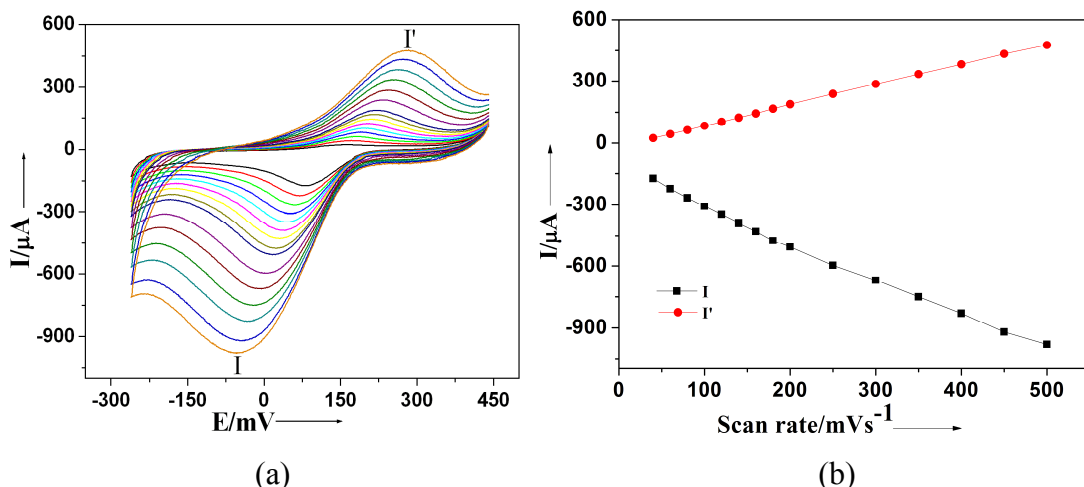


**Figure S10.** (a) Cyclic voltammograms of the **1**-CPE in the 1 M  $\text{H}_2\text{SO}_4$  aqueous solution at different scan rates (from inner to outer: 40, 60, 80, 100, 120, 140, 160, 180, 200, 250, 300, 350, 400, 450, 500  $\text{mV s}^{-1}$ ). (b) The dependence of cathodic peak (**I**) and anodic peak (**I'**) currents on scan rates.

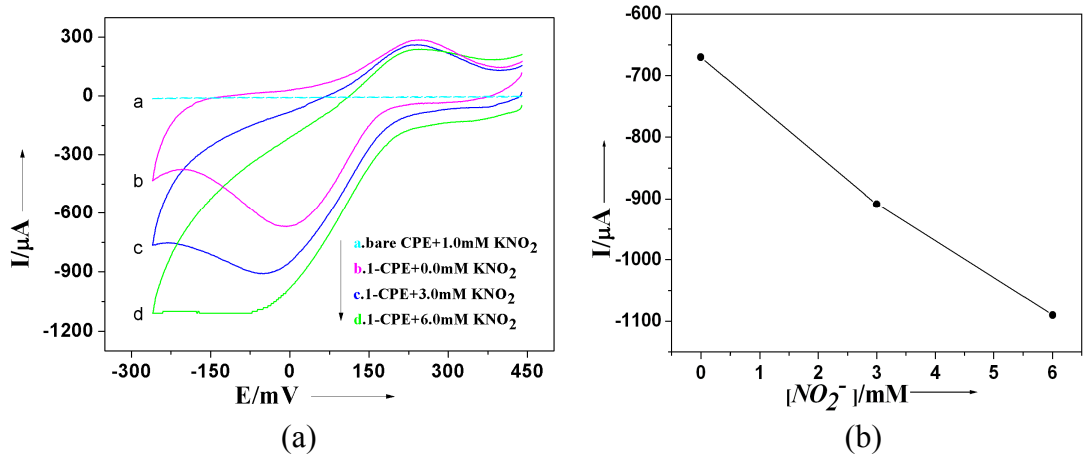


**Figure S11.** (a) Cyclic voltammograms of the 1-CPE in 1 M  $\text{H}_2\text{SO}_4$  aqueous solution containing 0.0–6.0 mM  $\text{KNO}_2$  and a bare CPE in 1.0 mM  $\text{KNO}_2$  + 1M  $\text{H}_2\text{SO}_4$  aqueous solution. Potentials vs SCE. Scan rate: 300  $\text{mVs}^{-1}$ . (b) The dependence of one cathodic peak (I) current on concentration of  $\text{NO}_2^-$ .

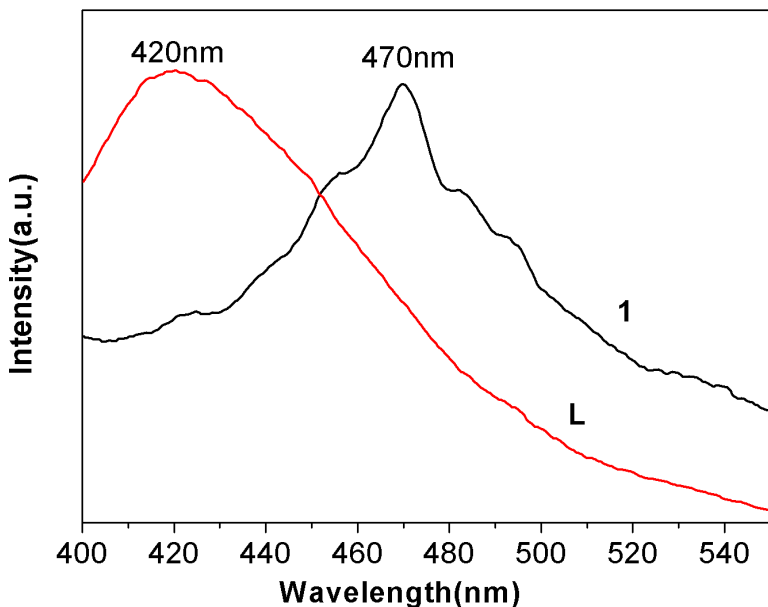


**Fig. S12.** Luminescence spectra of **1** and **L**.

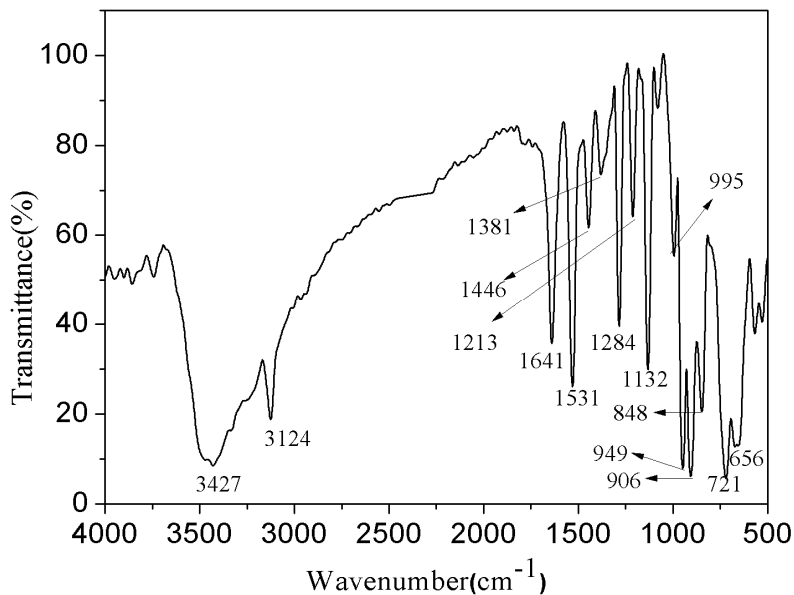


**Figure S13.** The IR spectrum of compound **1** exhibits the characteristic vibrations resulting from the  $\text{Mo}_8\text{O}_{26}^{4-}$  polyanion. In the spectrum of **1**, characteristic bands at 906, 848, 721, and 656  $\text{cm}^{-1}$  are attributed to the  $\nu(\text{Mo=O})$  or  $\nu(\text{Mo-O-Mo})$ . Bands in the regions of 1641–1132  $\text{cm}^{-1}$  are characteristic peaks of the **L** ligands.

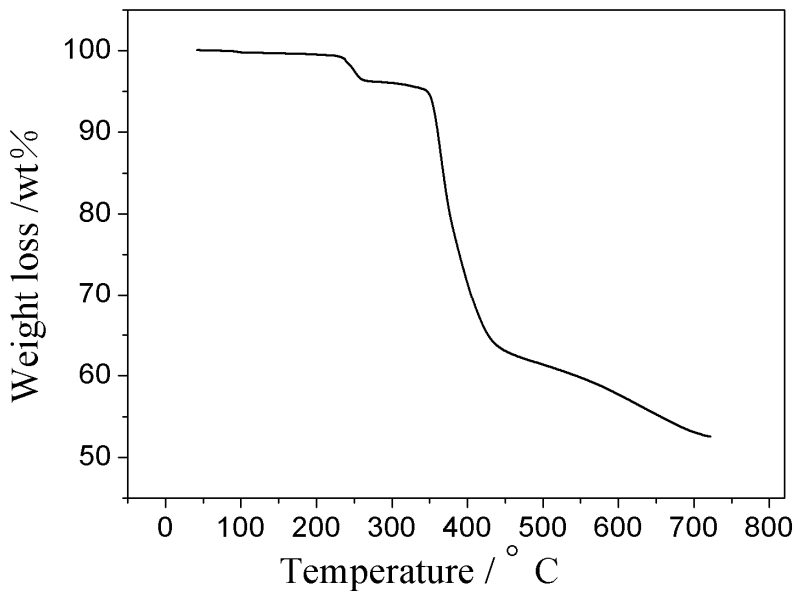


**Figure S14.** The TG curve for compound **1**. The TG curve exhibits two continuous weight loss stages in the range of 40–720  $^{\circ}\text{C}$  based on the samples consisting of numerous single crystals with a heating rate of  $10^{\circ}\text{C}\cdot\text{min}^{-1}$ . The weight loss of 3.0% (calcd 2.5%) from 220 to 260  $^{\circ}\text{C}$  corresponds to the loss of water molecules. After then, the decomposition of the framework occurs.

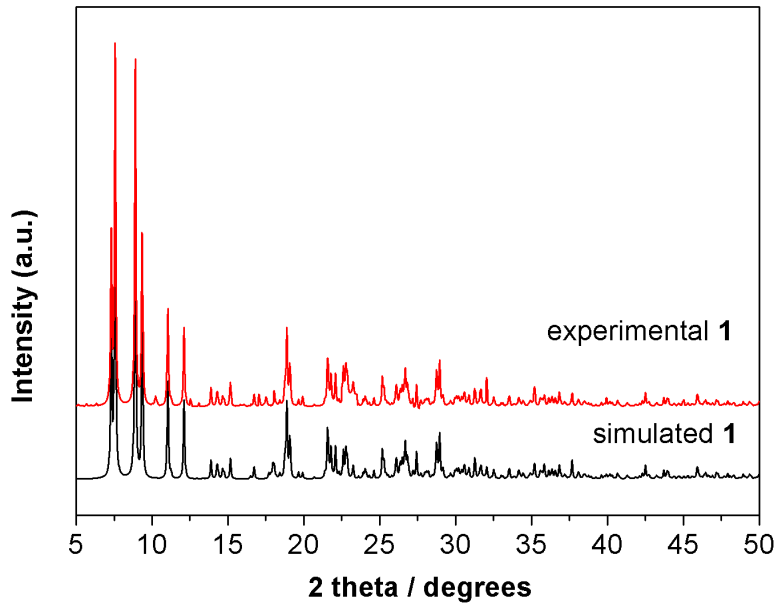


**Figure S15.** The simulated (black line) and experimental (red line) powder X-ray diffraction patterns for compound **1**. The diffraction peaks of both simulated and experimental patterns are in good agreement in the key positions, indicating the phase purities of the title compound. The difference in reflection intensities between the simulated and the experimental patterns is due to the different orientation of the crystals in the powder samples [1].

[1] A. X. Tian, J. Ying, J. Peng, J. Q. Sha, H. J. Pang, P. P. Zhang, Y. Chen, M. Zhu, Z. M. Su, *Cryst. Growth Des.* 2008, **8**, 3717;

**Table S1.** Crystal data and structure refinement summary for compound **1**.

Empirical formula	C <sub>16</sub> H <sub>28</sub> Mo <sub>4</sub> N <sub>12</sub> NiO <sub>15</sub>
Formula weight	1070.97
Temperature (K)	293(2)
Crystal system	Triclinic
Space group	P-1
<i>a</i> (Å)	10.599(5)
<i>b</i> (Å)	12.238(5)
<i>c</i> (Å)	13.468(5)
α (°)	73.105(5)
β (°)	70.024(5)
γ (°)	88.139(5)
Volume (Å <sup>3</sup> )	1566.6(11)
<i>Z</i>	2
<i>D<sub>calc</sub></i> (g/cm <sup>3</sup> )	2.270
Absorption coefficient (mm <sup>-1</sup> )	2.233
<i>F</i> (000)	1048
Crystal size (mm)	0.16 x 0.16 x 0.17
θ range (°)	2.03–25
Range of <i>h</i> , <i>k</i> , <i>l</i>	-12/12, -14/12, -15/26
Reflections collected	7907
Independent reflections	5423 ( <i>R</i> <sub>int</sub> = 0.0209)
Data / restraints / parameters	5423 / 0 / 440
Goodness-of-fit on <i>F</i> <sup>2</sup>	1.091
Final <i>R</i> indices [ <i>I</i> >2σ( <i>I</i> )]	<i>R</i> <sup>a</sup> = 0.0332, <i>wR</i> <sup>b</sup> = 0.0936
<i>R</i> indices (all data)	<i>R</i> <sup>a</sup> = 0.0467, <i>wR</i> <sup>b</sup> = 0.1172

<sup>a</sup>R<sub>1</sub> = Σ||*F*<sub>o</sub>|-|*F*<sub>c</sub>||/Σ|*F*<sub>o</sub>|; <sup>b</sup>wR<sub>2</sub> = Σ[w(*F*<sub>o</sub><sup>2</sup>-*F*<sub>c</sub><sup>2</sup>)<sup>2</sup>]/Σ[w(*F*<sub>o</sub><sup>2</sup>)<sup>2</sup>]<sup>1/2</sup>.

**Table S2.** Selected bond distances (Å) and angles (°) for compound **1**.

Ni(1)–O(13)#1	2.032(4)	Ni(2)–N(7)#2	2.093(5)
Ni(1)–O(13)#2	2.032(4)	Ni(2)–N(7)	2.093(5)
Ni(1)–N(6)#3	2.059(6)	Ni(2)–N(10)#2	2.099(6)
Ni(1)–N(6)	2.059(6)	Ni(2)–N(10)	2.099(6)
Ni(1)–O(1W)	2.124(4)	Ni(2)–O(9)	2.118(4)
Ni(1)–O(1W)#3	2.124(4)	Ni(2)–O(9)#2	2.118(4)
Mo(1)–O(7)	1.681(4)	Mo(3)–O(8)	1.715(4)
Mo(1)–O(13)	1.730(4)	Mo(3)–O(9)	1.728(4)
Mo(1)–O(6)#4	1.909(4)	Mo(3)–O(5)	1.855(4)
Mo(1)–O(5)	1.979(4)	Mo(3)–O(4)	2.108(4)
Mo(1)–O(1)	2.227(4)	Mo(3)–O(1)	2.221(4)
Mo(1)–O(3)#4	2.276(4)	Mo(3)–N(1)	2.248(5)
Mo(2)–O(10)	1.702(5)	Mo(4)–O(12)	1.711(4)
Mo(2)–O(11)	1.728(5)	Mo(4)–O(2)	1.757(4)
Mo(2)–O(4)	1.931(4)	Mo(4)–O(1)	1.890(4)
Mo(2)–O(6)	1.935(4)	Mo(4)–O(3)	1.921(4)
Mo(2)–O(3)	2.201(4)	Mo(4)–O(4)	2.194(4)
Mo(2)–O(2)#4	2.323(4)	Mo(4)–O(3)#4	2.476(4)
O(13)#1–Ni(1)–O(13)#2	180.000(1)	O(10)–Mo(2)–O(11)	104.1(2)
O(13)#1–Ni(1)–N(6)#3	89.7(2)	O(10)–Mo(2)–O(4)	104.2(2)
O(13)#2–Ni(1)–N(6)#3	90.3(2)	O(11)–Mo(2)–O(4)	97.1(2)
O(13)#1–Ni(1)–N(6)	90.3(2)	O(10)–Mo(2)–O(6)	101.4(2)
O(13)#2–Ni(1)–N(6)	89.7(2)	O(11)–Mo(2)–O(6)	96.49(19)
N(6)#3–Ni(1)–N(6)	180.0(3)	O(4)–Mo(2)–O(6)	146.96(18)
O(13)#1–Ni(1)–O(1W)	86.31(18)	O(10)–Mo(2)–O(3)	156.2(2)
O(13)#2–Ni(1)–O(1W)	93.69(18)	O(11)–Mo(2)–O(3)	99.63(19)
N(6)#3–Ni(1)–O(1W)	91.1(2)	O(4)–Mo(2)–O(3)	73.49(16)
N(6)–Ni(1)–O(1W)	88.9(2)	O(6)–Mo(2)–O(3)	74.61(17)
O(13)#1–Ni(1)–O(1W)#3	93.69(18)	O(10)–Mo(2)–O(2)#4	85.22(19)
O(13)#2–Ni(1)–O(1W)#3	86.31(18)	O(11)–Mo(2)–O(2)#4	170.49(19)

N(6)#3–Ni(1)–O(1W)#3	88.9(2)	O(4)–Mo(2)–O(2)#4	82.09(16)
N(6)–Ni(1)–O(1W)#3	91.1(2)	O(6)–Mo(2)–O(2)#4	79.64(16)
O(1W)–Ni(1)–O(1W)#3	180	O(3)–Mo(2)–O(2)#4	71.01(15)
N(7)#2–Ni(2)–N(7)	180.0(4)	O(8)–Mo(3)–O(9)	103.5(2)
N(7)#2–Ni(2)–N(10)#2	89.7(2)	O(8)–Mo(3)–O(5)	101.2(2)
N(7)–Ni(2)–N(10)#2	90.3(2)	O(9)–Mo(3)–O(5)	100.0(2)
N(7)#2–Ni(2)–N(10)	90.3(2)	O(8)–Mo(3)–O(4)	154.49(19)
N(7)–Ni(2)–N(10)	89.7(2)	O(9)–Mo(3)–O(4)	95.13(19)
N(10)#2–Ni(2)–N(10)	180.0(4)	O(5)–Mo(3)–O(4)	92.44(17)
N(7)#2–Ni(2)–O(9)	88.25(19)	O(8)–Mo(3)–O(1)	91.70(19)
N(7)–Ni(2)–O(9)	91.75(19)	O(9)–Mo(3)–O(1)	164.80(18)
N(10)#2–Ni(2)–O(9)	91.50(19)	O(5)–Mo(3)–O(1)	76.36(16)
N(10)–Ni(2)–O(9)	88.50(19)	O(4)–Mo(3)–O(1)	70.50(16)
N(7)#2–Ni(2)–O(9)#2	91.75(19)	O(8)–Mo(3)–N(1)	82.3(2)
N(7)–Ni(2)–O(9)#2	88.25(19)	O(9)–Mo(3)–N(1)	93.3(2)
N(10)#2–Ni(2)–O(9)#2	88.50(19)	O(5)–Mo(3)–N(1)	164.91(19)
N(10)–Ni(2)–O(9)#2	91.50(19)	O(4)–Mo(3)–N(1)	79.32(17)
O(9)–Ni(2)–O(9)#2	180.0(3)	O(1)–Mo(3)–N(1)	88.92(18)
O(7)–Mo(1)–O(13)	103.8(2)	O(12)–Mo(4)–O(2)	104.7(2)
O(7)–Mo(1)–O(6)#4	99.0(2)	O(12)–Mo(4)–O(1)	104.1(2)
O(13)–Mo(1)–O(6)#4	100.41(19)	O(2)–Mo(4)–O(1)	102.80(19)
O(7)–Mo(1)–O(5)	101.0(2)	O(12)–Mo(4)–O(3)	104.4(2)
O(13)–Mo(1)–O(5)	94.51(19)	O(2)–Mo(4)–O(3)	97.06(19)
O(6)#4–Mo(1)–O(5)	151.38(17)	O(1)–Mo(4)–O(3)	139.53(17)
O(7)–Mo(1)–O(1)	92.09(19)	O(12)–Mo(4)–O(4)	96.09(19)
O(13)–Mo(1)–O(1)	162.03(19)	O(2)–Mo(4)–O(4)	158.86(17)
O(6)#4–Mo(1)–O(1)	85.13(16)	O(1)–Mo(4)–O(4)	75.09(17)
O(5)–Mo(1)–O(1)	73.90(16)	O(3)–Mo(4)–O(4)	73.85(16)
O(7)–Mo(1)–O(3)#4	164.3(2)	O(12)–Mo(4)–O(3)#4	178.86(19)
O(13)–Mo(1)–O(3)#4	91.29(19)	O(2)–Mo(4)–O(3)#4	74.65(17)

---

O(6)#4–Mo(1)–O(3)#4	73.31(16)	O(1)–Mo(4)–O(3)#4	75.23(15)
O(5)–Mo(1)–O(3)#4	82.13(16)	O(3)–Mo(4)–O(3)#4	76.62(17)
O(1)–Mo(1)–O(3)#4	73.82(15)	O(4)–Mo(4)–O(3)#4	84.59(14)

---

Symmetry transformations used to generate equivalent atoms:**1:** #1 x, y + 1, z – 1, #2 –x, –y,  
–z; #3 –x, –y + 1, –z – 1, #4 –x, –y, –z + 1

---